AGU PUBLICATIONS

Geophysical Research Letters

RESEARCH LETTER

10.1002/2017GL076754

Key Points:

- The large-amplitude (up to 1.5 nT) hiss propagated toward higher latitudes in the plasmaspheric plumes
- The hiss wave power showed a similar frequency dependence to the modeled linear instability of hot electrons
- The hiss frequency-time spectrum consisted of a noisy band and a series of triggered rising tones

Correspondence to:
Z. Su,
szpe@mail.ustc.edu.cn

Citation:
Su, Z., Liu, N., Zheng, H., Wang, Y., & Wang, S. (2018). Large-amplitude extremely low frequency hiss waves in plasmaspheric plumes. *Geophysical Research Letters*, *45*, 565–577. https://doi.org/10.1002/2017GL076754

Received 10 DEC 2017
Accepted 12 JAN 2018
Accepted article online 16 JAN 2018
Published online 27 JAN 2018

Large-Amplitude Extremely Low Frequency Hiss Waves in Plasmaspheric Plumes

Zhenpeng Su[1,2], Nigang Liu[1,2,3], Huinan Zheng[1,2], Yuming Wang[1,2], and Shui Wang[1,2]

[1]CAS Key Laboratory of Geospace Environment, Department of Geophysics and Planetary Sciences, University of Science and Technology of China, Hefei, China, [2]Collaborative Innovation Center of Astronautical Science and Technology, University of Science and Technology of China, Hefei, China, [3]Mengcheng National Geophysical Observatory, School of Earth and Space Sciences, Hefei, China

Abstract Whistler-mode extremely low frequency hiss emissions commonly exist in the plasmasphere and the plasmaspheric plume and contribute to the precipitation loss of the radiation belt electrons. How these hiss waves are generated remains a critical unanswered question. Here we report the large-amplitude (up to 1.5 nT) hiss waves in the plasmaspheric plumes, nearly an order of magnitude stronger than previous observations. These waves are found to propagate toward higher latitudes, and the corresponding frequency dependence of wave power can be qualitatively (but not quantitatively) explained by the modeled linear instability of hot electrons near the equator. At the high-frequency end of hiss spectra, the discrete rising tones are shown to emerge, similar to the situation of whistler-mode chorus in the plasmatrough. These data and modeling suggest that these large-amplitude hiss waves were generated within the plasmaspheric plume probably through a combination of linear and nonlinear instabilities of hot electrons.

1. Introduction

In the plasmasphere and the plasmaspheric plume, the whistler-mode extremely low frequency (ELF, tens Hz to several kHz) hiss emissions commonly exist (Li et al., 2013; Malaspina et al., 2017; Russell et al., 1969; Summers et al., 2008; Thorne et al., 1973; Tsurutani et al., 2015; Yuan et al., 2012). The generation mechanism of ELF hiss remains under intense debate. Two classes of physical scenarios have been developed: (1) excitation by the hot electron instability inside the plasmasphere or the plasmaspheric plume ("internal generation") (Cornilleau-Wehrlin et al., 1993; Solomon et al., 1988; Thorne et al., 1979) and (2) origination from the whistlers associated with lightening flashes (Draganov et al., 1992; Green et al., 2005; Sonwalkar & Inan, 1989) or the whistler-mode chorus waves (Bortnik, Thorne, Meredith, 2008) in the plasmatrough ("external origination"). The main evidences for internal generation are the presence of hiss Poynting fluxes flowing from the equator toward higher latitudes (Kletzing et al., 2014; Laakso et al., 2015) and the highly coherent characteristics of hiss in the plasmaspheric bulges (Tsurutani et al., 2015). However, the gain from the linear instability was usually thought to be insufficient to explain the magnitude of typical plasmaspheric hiss waves (Church & Thorne, 1983; Huang et al., 1983). Inspired by the observations of short-time coherent hiss wave elements with rising and falling tones (Summers et al., 2014), Omura et al. (2015) have proposed the nonlinear instability theory to increase the wave growth rates. The experimental evidences for external origination are the strong correlation between chorus and hiss (Bortnik et al., 2009; Li et al., 2015), the occurrence of downward propagating chorus and upward propagating hiss at low altitudes (Tsurutani et al., 2012), the distribution characteristics of chorus and hiss with respect to the plasmapause (Malaspina et al., 2016; Meredith et al., 2013), and the simultaneous disappearances of chorus and hiss driven by interplanetary disturbances (Liu, Su, Gao, Zheng, et al., 2017; Liu, Su, Gao, Reeves, et al., 2017; Su et al., 2015). Moreover, there have been a series of ray tracing simulations showing that the chorus waves can enter the plasmasphere and evolve into the hiss band (Bortnik, Chen, Li, Thorne, & Horne, 2011; Bortnik, Chen, Li, Thorne, Meredith, & Horne, 2011; Chen et al., 2012a, 2012b).

ELF hiss waves are believed to contribute significantly to the precipitation loss of energetic electrons in the outer radiation belt (e.g., Li et al., 2007; Mourenas & Ripoll, 2012; Su et al., 2016) and the slot region (e.g., Albert, 1994; Abel & Thorne, 1998; Falkowski et al., 2017; Horne et al., 2003; He et al., 2016; Lyons & Thorne, 1973; Meredith et al., 2007; Thorne et al., 2013). This loss process was usually quantified in the framework of the quasi-linear theory (e.g., Lyons & Thorne, 1973; Ni et al., 2014; Shprits et al., 2009; Su et al., 2011). The time-averaged amplitude of hiss has been shown to be ~0.01 – 0.1 nT (Golden et al., 2012; Kim et al., 2015; Meredith et al., 2004; Spasojevic et al., 2015; Tsurutani et al., 2015), meeting the small amplitude assumption for the quasi-linear treatment (Horne & Thorne, 1998; Kennel & Engelmann, 1966; Kennel & Petschek, 1966; Summers et al., 1998). However, the time-averaged data may have underestimated significantly the instantaneous wave amplitudes (Tsurutani et al., 2009). In fact, there have been many reports of large-amplitude wave bursts in the inner magnetosphere: electromagnetic ion cyclotron waves (Bräysy et al., 1998; Erlandson & Ukhorskiy, 2001; Meredith et al., 2003; Su et al., 2016, 2017), chorus waves (e.g., Cattell et al., 2008; Cully, Bonnell, Ergun, et al., 2008; Santolík et al., 2014), magnetosonic waves (Tsurutani et al., 2014), and whistlers associated with transmitter or lightening (Breneman et al., 2011). These large-amplitude waves are able to nonlinearly scatter magnetospheric particles (Albert & Bortnik, 2009; Bortnik, Thorne, Inan, 2008; Omura et al., 2007; Omura & Zhao, 2012; Su et al., 2014; Summers & Omura, 2007; Wang et al., 2016; Zhu et al., 2012), deviating significantly from the quasi-linear prediction (Liu et al., 2012; Su et al., 2012, 2013). In contrast to the incoherent turbulence assumption for the quasi-linear treatment (Horne & Thorne, 1998; Kennel & Engelmann, 1966; Kennel & Petschek, 1966; Summers et al., 1998), the hiss waves have been found to be coherent under some conditions (Falkowski et al., 2017; Tsurutani et al., 2012, 2015). As shown in several theoretical calculations (Bellan, 2013; Lakhina et al., 2010; Tsurutani et al., 2009, 2013), these coherent hiss waves could cause much stronger scattering loss of electrons than the quasi-linear prediction.

In this letter, by analyzing the data from the Van Allen Probes (Radiation Belt Storm Probes, RBSP) (Mauk et al., 2013) and the Time History of Events and Macroscale Interactions during Substorm (THEMIS) satellites (Angelopoulos, 2008), we show that the large-amplitude (up to 1.5 nT) ELF hiss waves could be generated by the hot electron instability within the plasmaspheric plumes. These waves, consisting of a noisy band and a series of triggered rising tones, were about an order of magnitude stronger than the time-averaged hiss (~< 0.1 nT) (e.g., Golden et al., 2012; Meredith et al., 2004; Spasojevic et al., 2015) or the highly coherent hiss (up to 0.2 nT) (Tsurutani et al., 2015).

2. Data Analysis

We directly take the interplanetary and geomagnetic parameters from the OMNI database (King & Papitashvili, 2005) and analyze the magnetospheric waves based on the RBSP and THEMIS missions operating in the highly elliptical near-equatorial orbits. For the RBSP mission, we use the data sets of the Electric and Magnetic Field Instrument and Integrated Science (EMFISIS) suite (Kletzing et al., 2013), the Electric Field and Wave (EFW) instrument (Wygant et al., 2013), and the Energetic Particle, Composition and Thermal Plasma Suite (ECT) (Spence et al., 2013). The EMFISIS suite contains the tri-axial fluxgate magnetometer (MAG), the Waveform Receiver (WFR), and the High-Frequency Receiver (HFR). The MAG observes the local magnetic field, the WFR provides the wave spectral matrix in the frequency range from 10 Hz to 12 kHz and the continuous-burst waveforms with a 35 kHz sampling rate, and the HFR detects the upper hybrid band. The EFW measures the spacecraft potential and the low-frequency electric fields and waves. The upper hybrid frequency from HFR and the spacecraft potential from EFW allow the derivation of background plasma density (Kurth et al., 2014; Wygant et al., 2013). The ECT suite consists of the Helium Oxygen Proton Electron (HOPE) Mass Spectrometer (Funsten et al., 2013), the Magnetic Electron Ion Spectrometer (MagEIS) (Blake et al., 2013), and the Relativistic Electron Proton Telescope (Baker et al., 2013). The three instruments collectively cover the electron and ion spectra from eV to tens of MeV. For the THEMIS mission, we use the data sets of the Search Coil Magnetometer (SCM) (Le Contel et al., 2008) and the Electric Field Instrument (EFI) (Bonnell et al., 2008). The SCM and EFI measure the electromagnetic fields of waves in the frequency range from 0.1 Hz to 4 kHz. The Digital Fields Board (DFB) (Cully, Ergun, et al., 2008) processes the electromagnetic signals from SCM and EFI into the filter bank data of wave amplitudes for six spectral bands ranging from 2 Hz to 4 kHz. The EFI also measures the spacecraft potential, allowing the estimation of the background plasma density.

3. Event Overview

Figure 1 presents an overview of the large-amplitude hiss event on 1 December 2013. Before 09:00 UT, there were intermittent southward interplanetary magnetic fields and moderate substorms, allowing the erosion of plasmasphere (Goldstein et al., 2003; Lemaire & Gringauz, 1998) and the formation of plasmaspheric plume (Carpenter & Anderson, 1992; Goldstein et al., 2004; Nishida, 1966). RBSP-B was inside the high-density plasmasphere before 05:40 UT and after 11:30 UT and passed through a plasmaspheric plume with the sudden

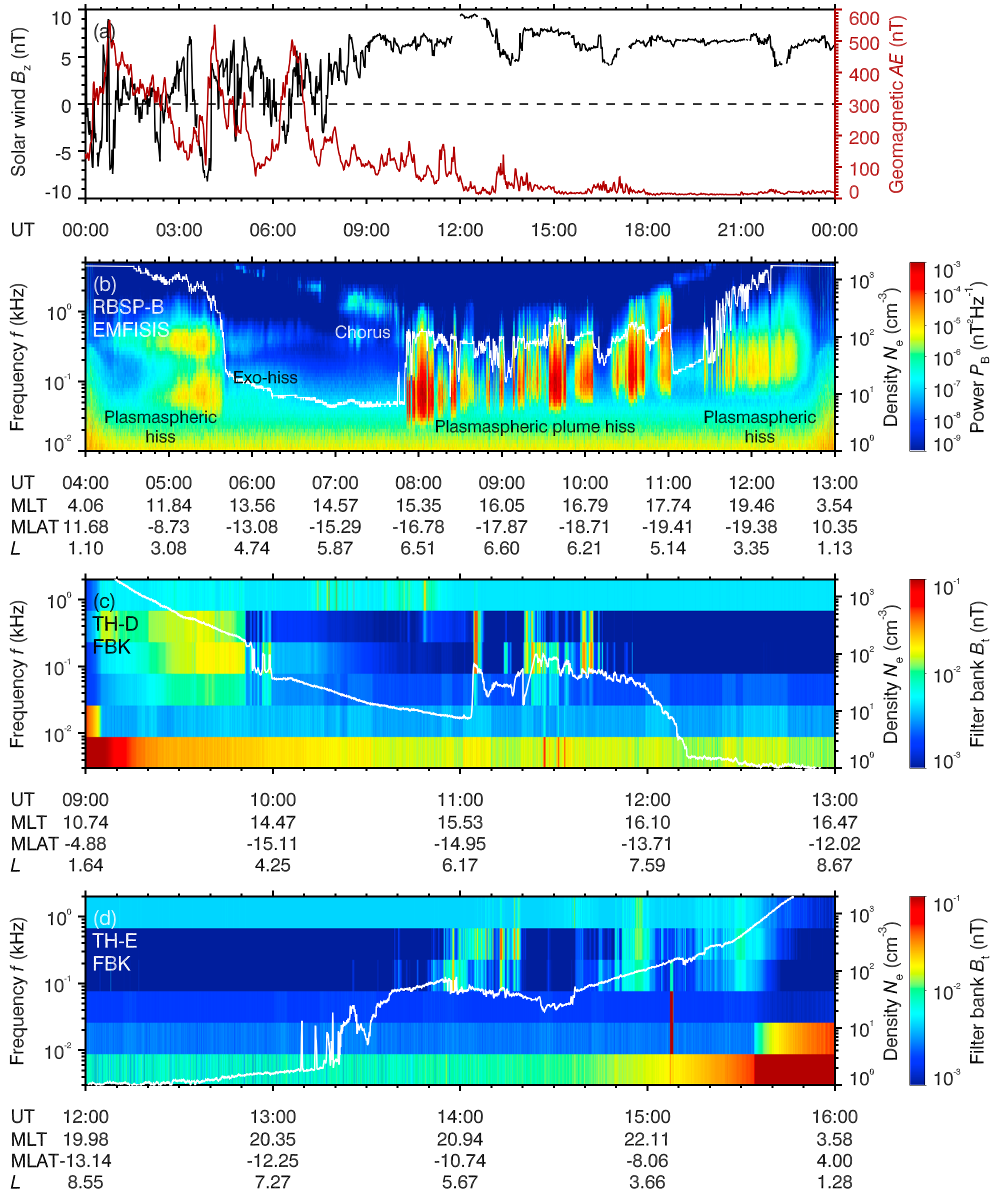

Figure 1. An overview of the large-amplitude hiss event on 1 December 2013: (a) solar wind magnetic field B_Z and substorm index *AE*; (b) wave power spectral density P_B (color coded) and cold electron density N_e (white line) observed by RBSP-B; (c, d) wave filter bank amplitude B_t (color coded) and cold electron density N_e (white line) observed by THEMIS-D and THEMIS-E.

enhancement of the cold electron density in the afternoon sector (MLT=15.0–18.0) during the time period from 07:50 UT to 11:05 UT. RBSP-B received hiss wave signals ranging from ~30 Hz to several kHz with intensity modulated by the ambient cold electron density (Chen et al., 2012). Particularly, the peak power spectral density of hiss waves reached 5×10^{-3} nT^2 Hz^{-1} in the plasmaspheric plume, approximately 2 orders of magnitude larger than that in the plasmasphere. In the remained time period, RBSP-B detected the whistler-mode chorus waves (Tsurutani & Smith, 1974) and exo-hiss waves (Thorne et al., 1973; Zhu et al., 2015) within the low-density plasmatrough. THEMIS-D went through the plasmapause at 09:50 UT and encountered the same plasmaspheric plume in the afternoon sector (MLT=15.6–16.2) during the time period from 11:05 UT to 12:10 UT. This plasmaspheric plume likely rotated into the premidnight sector (MLT=20.5–21.6), as observed by THEMIS-E in the time period from 13:10 UT to 14:25 UT. For both THEMIS satellites, the peak amplitudes of hiss were above 0.1 nT in the plasmaspheric plume, 5–10 times larger than that in the plasmasphere. It should be noted that the other satellites of RBSP and THEMIS missions failed to find the rotating plasmaspheric plume.

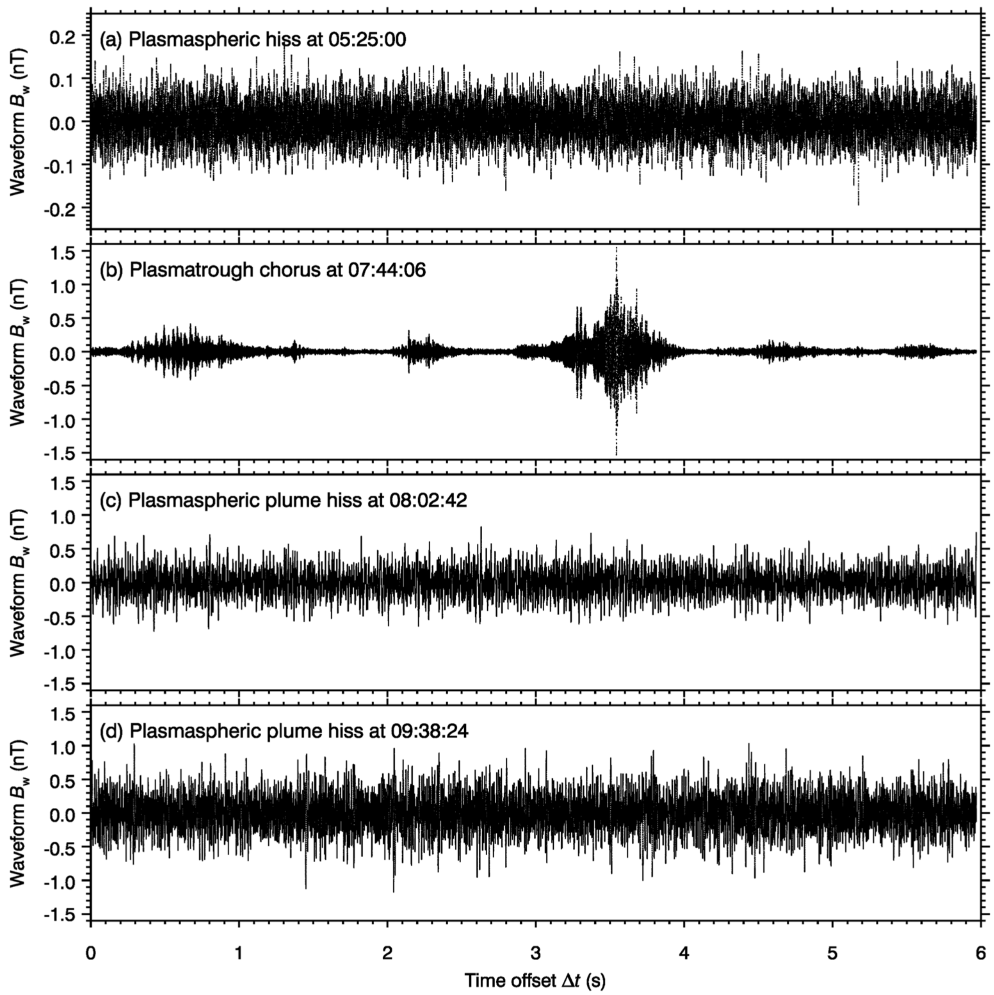

Figure 2. Waveform bursts of (a) plasmaspheric hiss, (b) plasmatrough chorus, and (c, d) plasmaspheric plume hiss detected by RBSP-B.

In the time range of interest, THEMIS-D and THEMIS-E did not provide the high-resolution waveform data. Figure 2 plots four representative waveform bursts observed by RBSP-B. In the plasmatrough (around 07:44:06 UT), chorus wave signals exhibited clear structures with the peak instantaneous amplitude of 1.5 nT, similar to the previously reported large-amplitude chorus elements (e.g., Cattell et al., 2008; Cully, Bonnell, Ergun, et al., 2008; Gao et al., 2016; Kellogg et al., 2011; Santolík et al., 2014; Wilson et al., 2011). In contrast, hiss wave signals always displayed no observable structures on the plotted timescale. In the plasmasphere (around 05:25:00 UT), the wave amplitudes were below 0.2 nT, generally comparable to the previous statistical results (Golden et al., 2012; Meredith et al., 2004; Spasojevic et al., 2015; Tsurutani et al., 2015). In the plasmaspheric plume, the hiss wave amplitudes became much larger. Around 08:02:42 UT, the instantaneous wave amplitudes exceptionally reached up to 0.7 nT. Around 09:38:24 UT, the instantaneous wave amplitudes frequently exceeded 0.5 nT and even reached up to 1.2 nT. These waves were much stronger than the time-averaged hiss ($\sim < 0.1$ nT) (e.g., Golden et al., 2012; Meredith et al., 2004; Spasojevic et al., 2015) or the highly coherent hiss (up to 0.2 nT) (Tsurutani et al., 2015). A question arises as to how these large-amplitude hiss waves were generated.

4. Generation Mechanism

Figure 3 shows the hot electron spectra and the wave propagation characteristics observed by RBSP-B. Applying the previously developed techniques (Santolík et al., 2002, 2003, 2010) on the observed spectral matrix, we determine wave vector direction, ellipticity of wave polarization, and Poynting vector. One can identify three types of whistler-mode waves (hiss, exo-hiss, and chorus) with the right-hand polarization

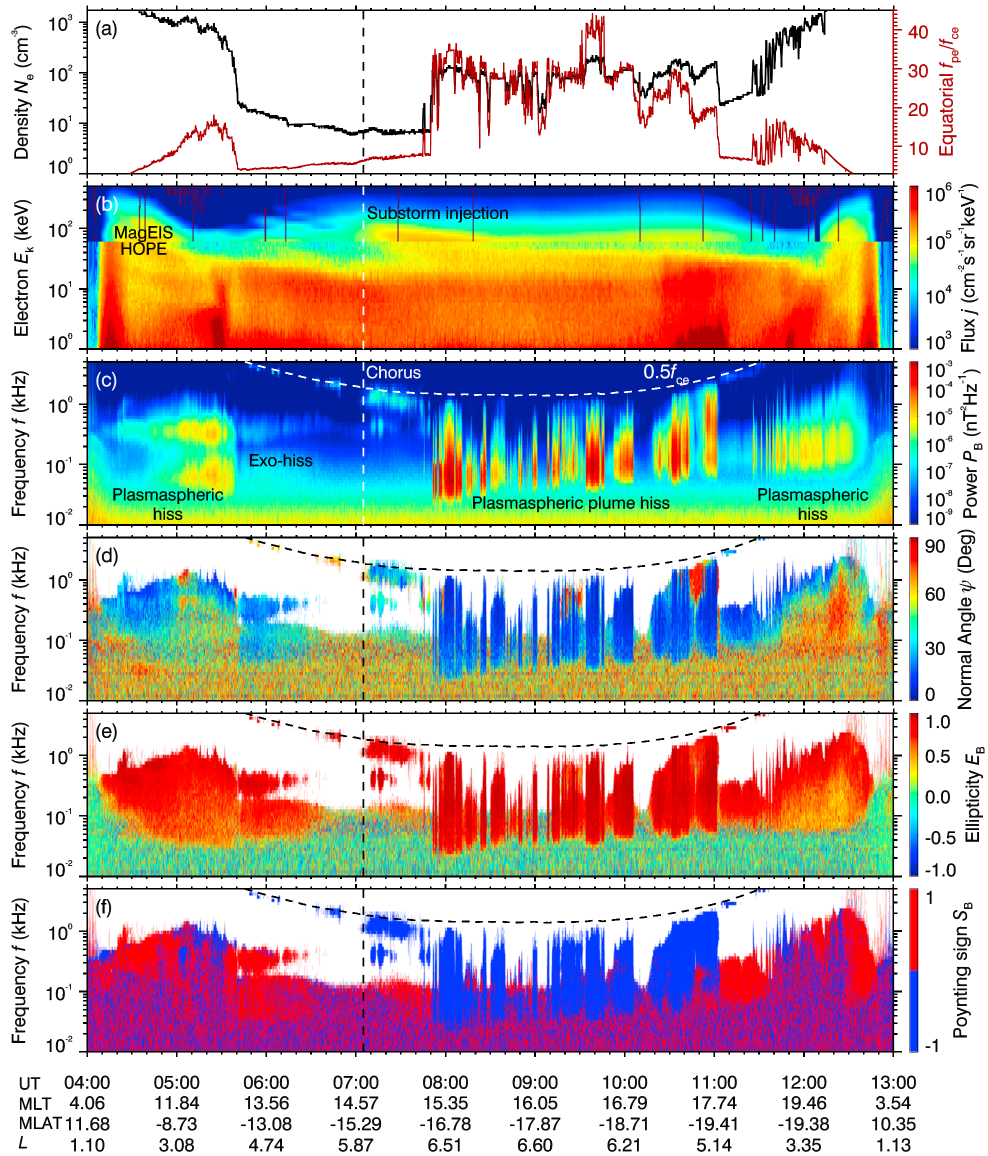

Figure 3. Generation and propagation of whistler-mode waves observed by RBSP-B: (a) cold electron density N_e and equatorial ratio of plasma frequency to electron gyrofrequency f_{pe}/f_{ce}; (b) hot electron flux j; (c) wave power spectral density P_B; (d) wave normal angle ψ; (e) wave ellipticity E_B; and (f) sign of the parallel component of the wave Poynting flux S_B (positive for parallel flowing and negative for antiparallel flowing). The vertical dashed line marks the front of the substorm injection.

(ellipticity values above 0.5). In the plasmasphere, hiss had bidirectional Poynting fluxes and randomly distributed normal angles, probably resulting from the wave bounce propagations (Bortnik, Chen, Li, Thorne, & Horne, 2011; Bortnik, Chen, Li, Thorne, Meredith, & Horne, 2011; Chen et al., 2012a, 2012b). The other whistler-mode waves in the plasmatrough and the plasmaspheric plume always exhibited the unidirectional Poynting fluxes. Exo-hiss propagated quasi-parallel to the background magnetic field toward the equator, supporting the previous hypothesis of leakage of plasmaspheric hiss into exo-hiss (Bortnik, Thorne, Meredith, 2008; Liu, Su, Gao, Zheng, et al., 2017; Thorne et al., 1973; Zhu et al., 2015). In contrast, both chorus and plume hiss propagated toward higher latitudes, which were likely generated by the electron cyclotron instability near the equator (LeDocq et al., 1998; Nunn et al., 1997; Omura et al., 2008). At 07:05 UT, the front of a substorm injection arrived at the location of RBSP-B ($L = 5.9$ and MLT = 15.0), and during the following time period, the substorm-induced enhancement of hot electrons could promote the amplification of chorus in the plasmatrough and hiss in the plasmaspheric plume.

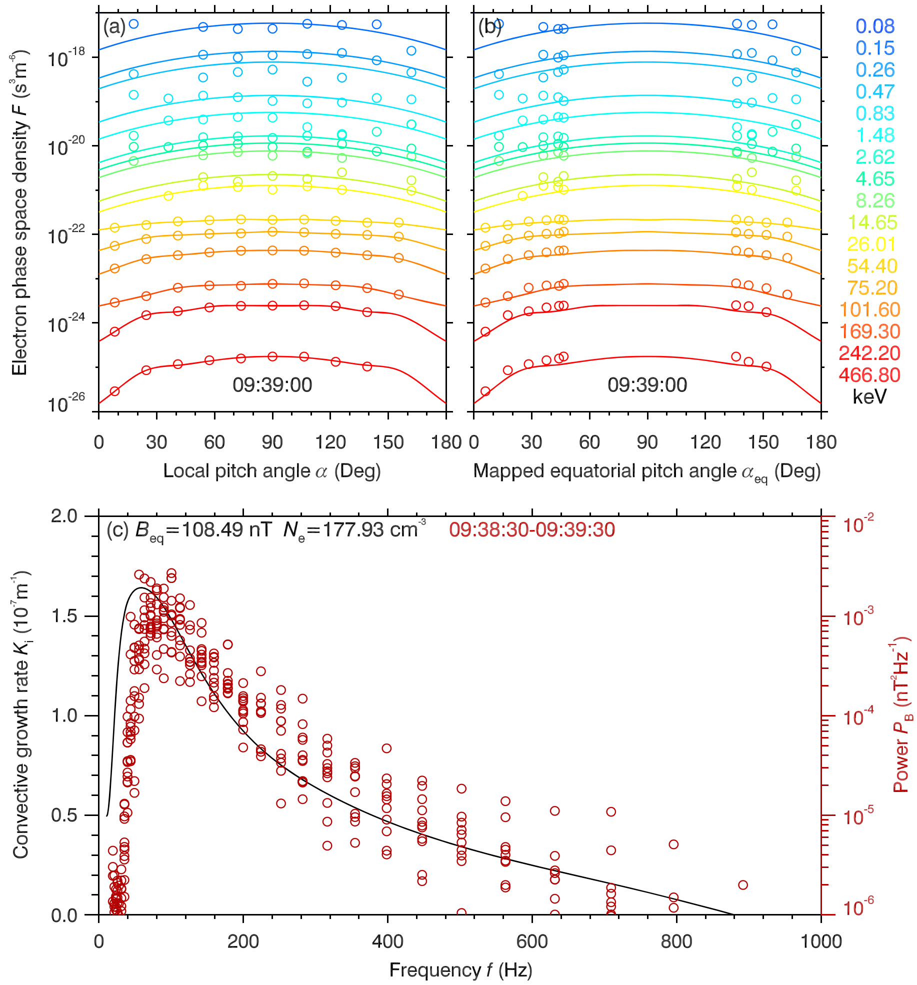

Figure 4. Whistler-wave instability for RBSP-B around 09:39 UT: (a) local and (b) equatorial pitch angle distributions (circles for data and solid lines for model); (c) dependence of wave convective growth rate K_i (solid line) and power spectral density P_B (circles) on frequency f.

The growth rates of magnetospheric whistler waves usually peaked at the magnetic equator. To perform the wave instability analysis at the equator, we have made the following assumptions: (1) the realistic ratio between equatorial and local magnetic fields equals the value from the TS04 geomagnetic field model (Tsyganenko & Sitnov, 2005), (2) there are no significant differences between the equatorial and local pitch angle distributions of hot electrons, and (3) the cold electron density is constant along the magnetic field line. Taking the limit that the wave temporal growth rate is much less than the real wave angular frequency, we can calculate the wave convective growth rate (Ashour-Abdalla & Kennel, 1978; Kennel & Engelmann, 1966) as

$$K_i = -\frac{D_i}{|\mathbf{V}_g| \frac{\partial D_r}{\partial \omega}}, \quad (1)$$

with the real D_r and imaginary D_i parts of the wave dispersion relation $D(\omega, \mathbf{k}) = 0$ (Chen et al., 2010, equations (A3)) and the wave group velocity $\mathbf{V}_g$.

Figure 4 displays the hot electron distributions and the wave convective growth rate around 09:39 UT. At this time moment, RBSP-B detected the large-amplitude hiss waves (Figure 2d). We obtain the electron phase space density model on the basis of local observations. For the MagEIS data above 30 keV, we approximate the observed pitch angle distribution by a smooth cubic spline at each energy channel. For the HOPE data below 30 keV, in order to remove the irregular fluctuations, we assume an analytical pitch angle distribution proportional to $\left(\frac{1+\sin\alpha}{2}\right)^2$ at each energy channel. At the equatorial plane, this model appears to be roughly in line with the available data mapped by the conservation of magnetic moment. According to the observations

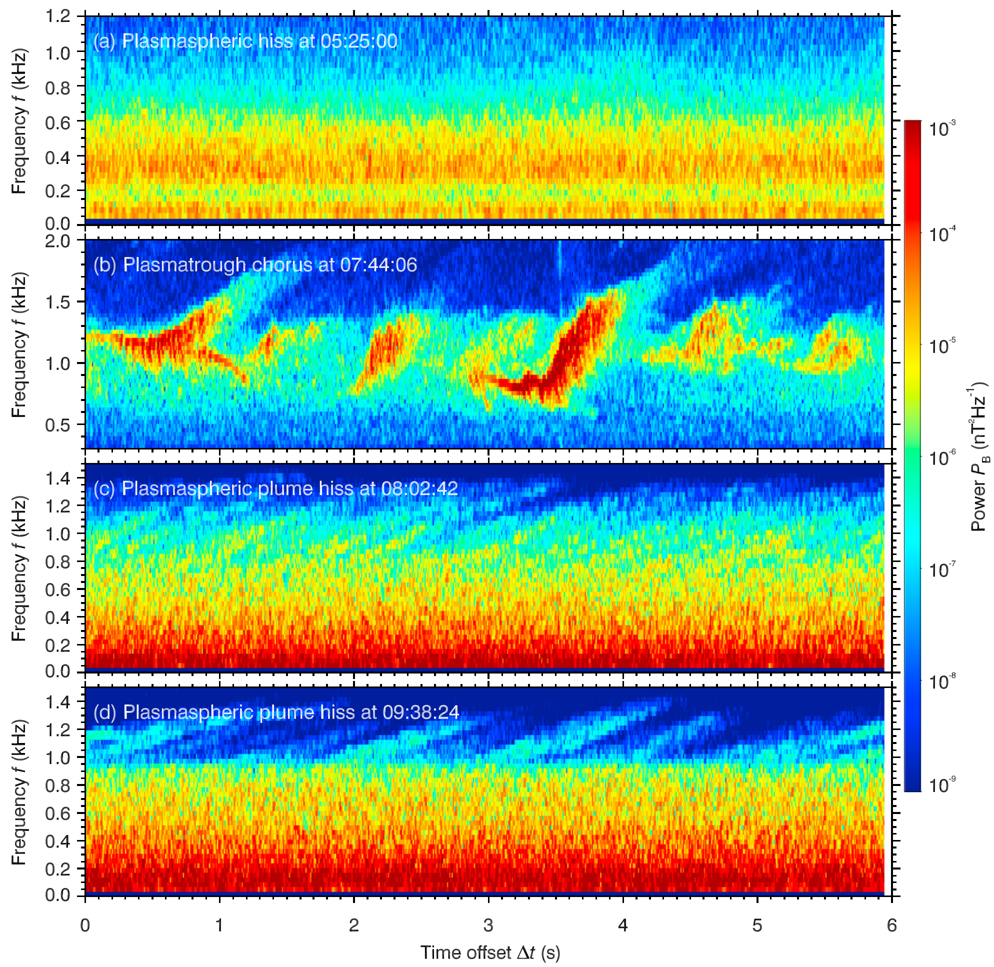

Figure 5. Burst frequency-time spectra of (a) plasmaspheric hiss, (b) plasmatrough chorus, and (c, d) plasmaspheric plume hiss detected by RBSP-B. The covered time periods are exactly same as those in Figure 2.

in Figures 1 and 3, we set the equatorial magnetic field of 108.49 nT and the cold electron density of 177.93 cm^{-3}. Under these plasma conditions, the parallel-propagating whistler-mode waves are able to grow over a wide frequency range from 20 Hz to 900 Hz. The obtained convective growth rate peaks at 60 Hz and exhibits a gradual decrease at the high-frequency end but a sharp decrease at the low-frequency end. These frequency-dependence characteristics of wave growth rate are found to be quite similar to those of wave power, supporting the generation of hiss waves by the hot electron instability near the equator in the plasmaspheric plume. However, corresponding to the large wave amplitude, the obtained linear growth rate ($\sim 10^{-7}$ m^{-1}) is quite small. There may be two explanations for this: (1) the model underestimates the electron temperature anisotropy in the absence of mapped data near the 90° equatorial pitch angle (Figure 4b); (2) after the linear instability, there was a nonlinear process with a much larger amplification rate (Omura et al., 2015).

Figure 5 compares wave frequency-time characteristics among four representative waveform bursts. The hiss emission in the plasmasphere (around 05:25:00 UT) appears to be structureless on the plotted timescale. In contrast, there were clear structures in the frequency-time spectra of the other waveforms. The chorus emission in the plasmatrough (around 07:44:06 UT) comprised rising tones, falling tones, and hooks, consistent with previous observations (Burtis & Helliwell, 1976; Li et al., 2012; Santolík et al., 2004; Smith & Nunn, 1998). The hiss emission in the plasmaspheric plume consisted of a noisy band and some rising tones, which was rarely reported in previous works. (Note that the whistler-mode chorus comprising a noisy band and a series of triggered rising tones has long been recognized in the low-density plasmatrough (Goldstein & Tsurutani, 1984; Tsurutani & Smith, 1974).) Around 08:02:42 UT, the dense rising tones swept over a range of 0.6–1.4 kHz on a timescale of 1 s. Around 09:38:24 UT, the rising tones became sparse and their sweeping frequency range was

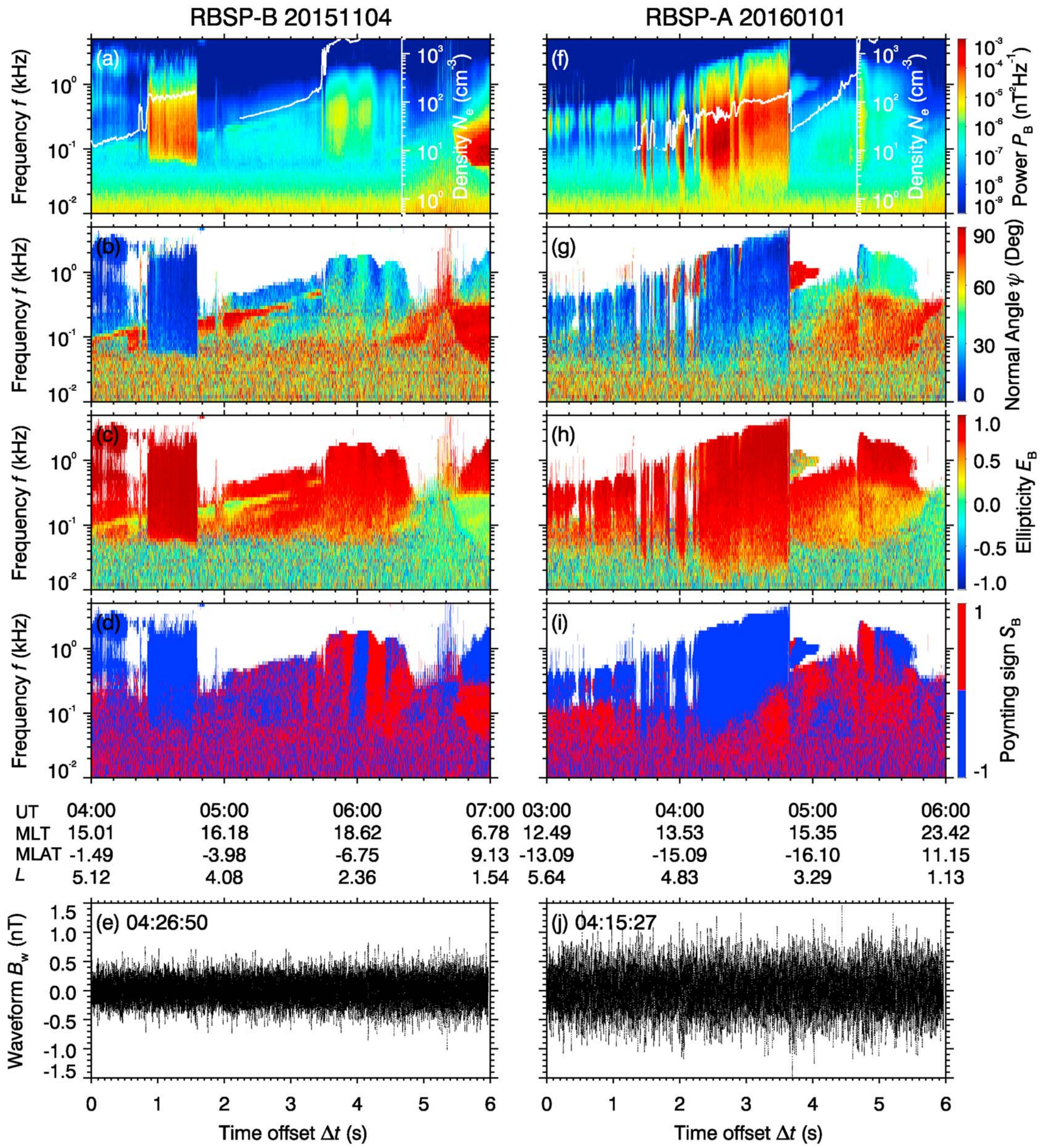

Figure 6. Overviews of the large-amplitude hiss events on 4 November 2015 and 1 January 2016: (a, f) wave power spectral density P_B; (b, g) wave normal angle ψ; (c, h) wave ellipticity E_B; (d, i) sign of the parallel component of wave Poynting flux S_B (positive for parallel flowing and negative for antiparallel flowing); and (e, j) waveform burst B_w of plasmaspheric plume hiss.

reduced to 0.9–1.4 kHz. Compared to the noisy band, these rising tones had much lower power and consequently were invisible in the waveforms (Figures 2c and 2d). These rising tones served as a direct evidence for the action of nonlinear process (Omura et al., 2015) in the plasmaspheric plume. Omura et al. (2015) have suggested that the discrete elements associated with nonlinear processes tend to have shorter duration periods at lower frequencies. As illustrated by Summers et al. (2014) and Nakamura et al. (2016), the noisy band might be a result of the superposition of many short-lived (∼10 ms) rising and falling tones.

5. Conclusions and Discussions

Whistler-mode ELF hiss emissions commonly exist in the plasmasphere and the plasmaspheric plume, whose generation mechanism remains under intense debate. Two classes of physical processes have been proposed: internal excitation (Omura et al., 2015; Thorne et al., 1979) and external origination (Bortnik, Thorne, Meredith, 2008). Here we analyze an interesting event of large-amplitude (∼nT) hiss waves observed by RBSP and THEMIS missions in a plasmaspheric plume on 1 December 2013. These waves had the Poynting fluxes flowing toward higher latitudes, and their power showed a similar frequency dependence to the modeled linear instability of hot electrons at the equator. Similar to the chorus in the low-density plasmatrough (Goldstein & Tsurutani, 1984; Tsurutani & Smith, 1974), the hiss exhibited a noisy band and a series of triggered rising tones in the frequency-time spectrum. Our observations and simulations tend to support the internal excitation of the large-amplitude plasmaspheric plume hiss by a combination of linear and nonlinear instabilities of hot electrons (Omura et al., 2015; Thorne et al., 1979). However, the calculated linear growth rates (Thorne et al., 1979) appear to be quite weak, and whether the additional nonlinear amplification process (Omura et al., 2015) can reproduce the large-amplitude hiss needs to be quantitatively examined in the future.

Such large-amplitude ELF hiss waves generated inside the plasmaspheric plume can be frequently observed. Another two examples observed by RBSP mission on 4 November 2015 and 1 January 2016 are given in Figure 6. In these plumes at $3 < L < 5$, the hiss waves had the instantaneous amplitudes up to 1.5 nT and propagated away from the equator toward higher latitudes. Laakso et al. (2015) have suggested the origination of plasmaspheric hiss from the plasmaspheric plume, on the basis of CLUSTER observations that the hiss emissions propagated away from the equator in the plumes but toward the equator at lower L shells inside the plasmasphere. On the basis of Polar observations, Tsurutani et al. (2012) found the frequency dependence of hiss Poynting fluxes in the low-altitude plasmasphere. The low-frequency (~360–800 Hz) part propagated upward and the high-frequency (~1.2 kHz) part propagated downward. The upward propagating hiss was interpreted as the chorus rays refracted into the plasmasphere (Tsurutani et al., 2012), and the downward propagating hiss might be generated at the equator within the plasmasphere (similar to the situation reported here). Different from the observations of Tsurutani et al. (2012) and Laakso et al. (2015), the plasmaspheric hiss of our study exhibited the bidirectional Poynting fluxes, approximately independent of the frequency (Figure 3f). These results suggest that the relationship between hiss waves in the plasmasphere and in the plasmaspheric plume remains unclear, and the relative importance of internal and external generation mechanisms for hiss waves in the plasmasphere body needs to be further investigated.

ELF hiss waves are frequently invoked to explain the precipitation loss of energetic electrons in the outer radiation belt and in the slot region (e.g., Breneman et al., 2015; Falkowski et al., 2017; Lyons & Thorne, 1973; Meredith et al., 2007; Summers et al., 2008; Thorne et al., 2013). This loss process has been usually quantified in the framework of the quasi-linear theory with an assumption of the incoherent weak wave turbulence. Previous theoretical works (Bellan, 2013; Lakhina et al., 2010; Tsurutani et al., 2009, 2013) emphasized that the coherent hiss (Falkowski et al., 2017; Tsurutani et al., 2012, 2015) could cause much stronger scattering loss than the quasi-linear prediction. The quasi-coherent hiss, probably originating from the plasmatrough chorus, was considered (Falkowski et al., 2017) an alternative explanation for the generation of the radiation belt slot region. In our study, the weak rising tones should be coherent on a timescale of ~1 s (Figures 5c and 5d), and the intense noisy band may be interpreted as a superposition of many short-lived (~10 ms) coherent rising and falling tones at different frequencies (Nakamura et al., 2016; Summers et al., 2014; Tsurutani et al., 2015). Several test particle simulations suggested that a large-amplitude spectrum of waves could cause the nonlinear electron scattering (e.g., Liu et al., 2012), analogous to the situation of a large-amplitude monochromatic wave (e.g., Albert & Bortnik, 2009; Omura & Zhao, 2012). Future works should test the applicability of the traditional quasi-linear theory to the hiss-driven radiation belt behaviors under different conditions of wave coherence and amplitude.

Acknowledgments
We acknowledge EMFISIS, ECT, and EFW teams for the use of RBSP data and acknowledge SCM, EFI, and DFB teams for the use of THEMIS data. Data are available from the following websites: http://emfisis.physics.uiowa.edu/Flight/, http://www.rbsp-ect.lanl.gov/data_pub/, http://www.space.umn.edu/rbspefw-data/, and http://cdaweb.gsfc.nasa.gov/cdaweb/istp_public/. This work was supported by the National Natural Science Foundation of China grants 41774170, 41631071, 41422405, 41274174, 41174125, 41131065, 41421063, 41231066 and 41304134; the Chinese Academy of Sciences grants KZCX2-EW-QN510 and KZZD-EW-01-4; the CAS Key Research Program of Frontier Sciences grant QYZDB-SSW-DQC015; the National Key Basic Research Special Foundation of China grant 2011CB811403; and the Fundamental Research Funds for the Central Universities grant WK2080000077.

References

Abel, B., & Thorne, R. M. (1998). Electron scattering loss in Earth's inner magnetosphere 1. Dominant physical processes. *Journal of Geophysical Research*, *103*, 2385–2396. https://doi.org/10.1029/97JA02919

Albert, J. M. (1994). Quasi-linear pitch angle diffusion coefficients: Retaining high harmonics. *Journal of Geophysical Research*, *99*, 23,741–23,745. https://doi.org/10.1029/94JA02345

Albert, J. M., & Bortnik, J. (2009). Nonlinear interaction of radiation belt electrons with electromagnetic ion cyclotron waves. *Geophysical Research Letters*, *36*, L12110. https://doi.org/10.1029/2009GL038904

Angelopoulos, V. (2008). The THEMIS mission. *Space Science Reviews*, *141*, 5–34. https://doi.org/10.1007/ s11214-008-9336-1

Ashour-Abdalla, M., & Kennel, C. (1978). Nonconvective and convective electron cyclotron harmonic instabilities. *Journal of Geophysical Research*, *83*(A4), 1531–1543. https://doi.org/10.1029/JA083iA04p01531

Baker, D. N., Kanekal, S. G., Hoxie, V. C., Batiste, S., Bolton, M., Li, X., … Friedel, R. (2013). The Relativistic Electron-Proton Telescope (REPT) instrument on board the Radiation Belt Storm Probes (RBSP) spacecraft: Characterization of Earth's radiation belt high-energy particle populations. *Space Science Reviews*, *179*, 337–381. https://doi.org/10.1007/s11214-012-9950-9

Bellan, P. M. (2013). Pitch angle scattering of an energetic magnetized particle by a circularly polarized electromagnetic wave. *Physics of Plasmas*, *20*(4), 042117. https://doi.org/10.1063/1.4801055

Blake, J. B., Carranza, P. A., Claudepierre, S. G., Clemmons, J. H., Crain, W. R., Dotan, Y., … Zakrzewski, M. P. (2013). The magnetic electron ion spectrometer (MagEIS) instruments aboard the Radiation Belt Storm Probes (RBSP) spacecraft. *Space Science Reviews*, *179*, 383–421. https://doi.org/10.1007/ s11214-013-9991-8

Bonnell, J. W., Mozer, F. S., Delory, G. T., Hull, A. J., Ergun, R. E., Cully, C. M., … Harvey, P. R. (2008). The Electric Field Instrument (EFI) for THEMIS. *Space Science Reviews*, *141*, 303–341. https://doi.org/10.1007/s11214-008-9469-2

Bortnik, J., Thorne, R. M., & Inan, U. S. (2008). Nonlinear interaction of energetic electrons with large amplitude chorus. *Geophysical Research Letters*, *35*, L21102. https://doi.org/10.1029/2008GL035500

Bortnik, J., Thorne, R. M., & Meredith, N. P. (2008). The unexpected origin of plasmaspheric hiss from discrete chorus emissions. *Nature*, *452*, 62–66. https://doi.org/10.1038/nature06741

Bortnik, J., Li, W., Thorne, R. M., Angelopoulos, V., Cully, C., Bonnell, J., … Roux, A. (2009). An observation linking the origin of plasmaspheric hiss to discrete chorus emissions. *Science*, *324*, 775–778. https://doi.org/10.1126/science.1171273

Bortnik, J., Chen, L., Li, W., Thorne, R. M., & Horne, R. B. (2011). Modeling the evolution of chorus waves into plasmaspheric hiss. *Journal of Geophysical Research*, *116*, A08221. https://doi.org/10.1029/2011JA016499

Bortnik, J., Chen, L., Li, W., Thorne, R. M., Meredith, N. P., & Horne, R. B. (2011). Modeling the wave power distribution and characteristics of plasmaspheric hiss. *Journal of Geophysical Research*, *116*, A12209. https://doi.org/10.1029/2011JA016862

Bräysy, T., Mursula, K., & Marklund, G. (1998). Ion cyclotron waves during a great magnetic storm observed by Freja double-probe electric field instrument. *Journal of Geophysical Research*, *103*, 4145–4156. https://doi.org/10.1029/97JA02820

Breneman, A., Cattell, C., Wygant, J., Kersten, K., Wilson, L. B., Schreiner III, S., … Goetz, K. (2011). Large-amplitude transmitter-associated and lightning-associated whistler waves in the Earth's inner plasmasphere at $L<2$. *Journal of Geophysical Research*, *116*, A06310. https://doi.org/10.1029/2010JA016288

Breneman, A., Halford, A., Millan, R., McCarthy, M., Fennell, J., Sample, J., … Kletzing, C. (2015). Global-scale coherence modulation of radiation-belt electron loss from plasmaspheric hiss. *Nature*, *523*, 193–195. https://doi.org/10.1038/nature14515

Burtis, W. J., & Helliwell, R. A. (1976). Magnetospheric chorus—Occurrence patterns and normalized frequency. *Planetary and Space Science*, *24*, 1007–1024. https://doi.org/10.1016/0032-0633(76)90119-7

Carpenter, D. L., & Anderson, R. R. (1992). An ISEE/whistler model of equatorial electron density in the magnetosphere. *Journal of Geophysical Research*, *97*, 1097–1108.

Cattell, C., Wygant, J. R., Goetz, K., Kersten, K., Kellogg, P. J., von Rosenvinge, T., … Russell, C. T. (2008). Discovery of very large amplitude whistler-mode waves in Earth's radiation belts. *Geophysical Research Letters*, *35*, L01105. https://doi.org/10.1029/2007GL032009

Chen, L., Thorne, R. M., Jordanova, V. K., Wang, C.-P., Gkioulidou, M., Lyons, L., & Horne, R. B. (2010). Global simulation of EMIC wave excitation during the 21 April 2001 storm from coupled RCM-RAM-HOTRAY modeling. *Journal of Geophysical Research*, *115*, A07209. https://doi.org/10.1029/2009JA015075

Chen, L., Bortnik, J., Li, W., Thorne, R. M., & Horne, R. B. (2012a). Modeling the properties of plasmaspheric hiss: 1. Dependence on chorus wave emission. *Journal of Geophysical Research*, *117*, A05201. https://doi.org/10.1029/2011JA017201

Chen, L., Bortnik, J., Li, W., Thorne, R. M., & Horne, R. B. (2012b). Modeling the properties of plasmaspheric hiss: 2. Dependence on the plasma density distribution. *Journal of Geophysical Research*, *117*, A05202. https://doi.org/10.1029/2011JA017202

Chen, L., Thorne, R. M., Li, W., Bortnik, J., Turner, D., & Angelopoulos, V. (2012). Modulation of plasmaspheric hiss intensity by thermal plasma density structure. *Geophysical Research Letters*, *39*, L14103. https://doi.org/10.1029/2012GL052308

Church, S. R., & Thorne, R. M. (1983). On the origin of plasmaspheric hiss—Ray path integrated amplification. *Journal of Geophysical Research*, *88*, 7941–7957. https://doi.org/10.1029/JA088iA10p07941

Cornilleau-Wehrlin, N., Solomon, J., Korth, A., & Kremser, G. (1993). Generation mechanism of plasmaspheric ELF/VLF hiss: A statistical study from GEOS 1 data. *Journal of Geophysical Research*, *98*, 21,471–21,480. https://doi.org/10.1029/93JA01919

Cully, C. M., Bonnell, J. W., & Ergun, R. E. (2008). THEMIS observations of long-lived regions of large-amplitude whistler waves in the inner magnetosphere. *Geophysical Research Letters*, *35*, L17S16. https://doi.org/10.1029/2008GL033643

Cully, C. M., Ergun, R. E., Stevens, K., Nammari, A., & Westfall, J. (2008). The THEMIS Digital Fields Board. *Space Science Reviews*, *141*, 343–355. https://doi.org/10.1007/s11214-008-9417-1

Draganov, A. B., Inan, U. S., Sonwalkar, V. S., & Bell, T. F. (1992). Magnetospherically reflected whistlers as a source of plasmaspheric hiss. *Geophysical Research Letters*, *19*, 233–236. https://doi.org/10.1029/91GL03167

Erlandson, R. E., & Ukhorskiy, A. J. (2001). Observations of electromagnetic ion cyclotron waves during geomagnetic storms: Wave occurrence and pitch angle scattering. *Journal of Geophysical Research*, *106*, 3883–3896. https://doi.org/10.1029/2000JA000083

Falkowski, B. J., Tsurutani, B. T., Lakhina, G. S., & Pickett, J. S. (2017). Two sources of dayside intense, quasi-coherent plasmaspheric hiss: A new mechanism for the slot region? *Journal of Geophysical Research: Space Physics*, *122*, 1643–1657. https://doi.org/10.1002/2016JA023289

Funsten, H. O., Skoug, R. M., Guthrie, A. A., MacDonald, E. A., Baldonado, J. R., Harper, R. W., … Chen, J. (2013). Helium, Oxygen, Proton, and Electron (HOPE) mass spectrometer for the Radiation Belt Storm Probes mission. *Space Science Reviews*, *179*, 423–484. https://doi.org/10.1007/ s11214-013-9968-7

Gao, Z., Su, Z., Zhu, H., Xiao, F., Zheng, H., Wang, Y., … Wang, S. (2016). Intense low-frequency chorus waves observed by Van Allen Probes: Fine structures and potential effect on radiation belt electrons. *Geophysical Research Letters*, *43*, 967–977. https://doi.org/10.1002/2016GL067687

Golden, D. I., Spasojevic, M., Li, W., & Nishimura, Y. (2012). Statistical modeling of plasmaspheric hiss amplitude using solar wind measurements and geomagnetic indices. *Geophysical Research Letters*, *39*, L06103. https://doi.org/10.1029/2012GL051185

Goldstein, B. E., & Tsurutani, B. T. (1984). Wave normal directions of chorus near the equatorial source region. *Journal of Geophysical Research*, *89*, 2789–2810. https://doi.org/10.1029/JA089iA05p02789

Goldstein, J., Sandel, B. R., Forrester, W. T., & Reiff, P. H. (2003). IMF-driven plasmasphere erosion of 10 July 2000. *Geophysical Research Letters*, *30*(3), 1146. https://doi.org/10.1029/2002GL016478

Goldstein, J., Sandel, B. R., Thomsen, M. F., Spasojević, M., & Reiff, P. H. (2004). Simultaneous remote sensing and in situ observations of plasmaspheric drainage plumes. *Journal of Geophysical Research*, *109*, A03202. https://doi.org/10.1029/2003JA010281

Green, J. L., Boardsen, S., Garcia, L., Taylor, W. W. L., Fung, S. F., & Reinisch, B. W. (2005). On the origin of whistler mode radiation in the plasmasphere. *Journal of Geophysical Research*, *110*, A03201. https://doi.org/10.1029/2004JA010495

He, Z., Yan, Q., Chu, Y., & Cao, Y. (2016). Wave-driven gradual loss of energetic electrons in the slot region. *Journal of Geophysical Research: Space Physics*, *121*, 8614–8623. https://doi.org/10.1002/2016JA023087

Horne, R. B., & Thorne, R. M. (1998). Potential waves for relativistic electron scattering and stochastic acceleration during magnetic storms. *Geophysical Research Letters*, *25*, 3011–3014. https://doi.org/10.1029/98GL01002

Horne, R. B., Meredith, N. P., Thorne, R. M., Heynderickx, D., Iles, R. H. A., & Anderson, R. R. (2003). Evolution of energetic electron pitch angle distributions during storm time electron acceleration to megaelectronvolt energies. *Journal of Geophysical Research*, *108*(A1), 1016. https://doi.org/10.1029/2001JA009165

Huang, C. Y., Goertz, C. K., & Anderson, R. R. (1983). A theoretical study of plasmaspheric hiss generation. *Journal of Geophysical Research*, *88*, 7927–7940. https://doi.org/10.1029/JA088iA10p07927

Kellogg, P., Cattell, C., Goetz, K., Monson, S., & Wilson, L. (2011). Large amplitude whistlers in the magnetosphere observed with wind-waves. *Journal of Geophysical Research*, *116*, A09224. https://doi.org/10.1029/2010JA015919

Kennel, C. F., & Engelmann, F. (1966). Velocity space diffusion from weak plasma turbulence in a magnetic field. *Physics of Fluids*, *9*, 2377–2388. https://doi.org/10.1063/1.1761629

Kennel, C. F., & Petschek, H. E. (1966). Limit on stably trapped particle fluxes. *Journal of Geophysical Research*, *71*, 1–28. https://doi.org/10.1029/JZ071i001p00001

Kim, K.-C., Lee, D.-Y., & Shprits, Y. (2015). Dependence of plasmaspheric hiss on solar wind parameters and geomagnetic activity and modeling of its global distribution. *Journal of Geophysical Research: Space Physics*, *120*, 1153–1167. https://doi.org/10.1002/2014JA020687

King, J. H., & Papitashvili, N. E. (2005). Solar wind spatial scales in and comparisons of hourly Wind and ACE plasma and magnetic field data. *Journal of Geophysical Research*, *110*, A02104. https://doi.org/10.1029/2004JA010649

Kletzing, C., Kurth, W. S., Bounds, S. R., Hospodarsky, G. B., Santolik, O., Wygant, J. R., … Summers, D. (2014). Evidence for significant local generation of plasmaspheric hiss. Abstract SM14A-09 Presented at the 2014 AGU Fall Meeting, San Francisco, CA, December 15-19.

Kletzing, C. A., Kurth, W. S., Acuna, M., MacDowall, R. J., Torbert, R. B., Averkamp, T., … Tyler, J. (2013). The Electric and Magnetic Field Instrument Suite and Integrated Science (EMFISIS) on RBSP. *Space Science Reviews*, *179*, 127–181. https://doi.org/10.1007/s11214-013-9993-6

Kurth, W. S., Pascuale, S. D., Faden, J. B., Kletzing, C. A., Hospodarsky, G. B., Thaller, S., & Wygant, J. R. (2014). Electron densities inferred from plasma wave spectra obtained by the waves instrument on Van Allen Probes. *Journal of Geophysical Research: Space Physics*, *120*, 904–914. https://doi.org/10.1002/2014JA020857

Laakso, H., Santolik, O., Horne, R., Kolmasová, I., Escoubet, P., Masson, A., & Taylor, M. (2015). Identifying the source region of plasmaspheric hiss. *Geophysical Research Letters*, *42*, 3141–3149. https://doi.org/10.1002/2015GL063755

Lakhina, G. S., Tsurutani, B. T., Verkhoglyadova, O. P., & Pickett, J. S. (2010). Pitch angle transport of electrons due to cyclotron interactions with the coherent chorus subelements. *Journal of Geophysical Research*, *115*, A00F15. https://doi.org/10.1029/2009JA014885

Le Contel, O., Roux, A., Robert, P., Coillot, C., Bouabdellah, A., de La Porte, B., … Larson, D. (2008). First results of the THEMIS Search Coil Magnetometers. *Space Science Reviews*, *141*, 509–534. https://doi.org/10.1007/s11214-008-9371-y

LeDocq, M. J., Gurnett, D. A., & Hospodarsky, G. B. (1998). Chorus source locations from VLF Poynting flux measurements with the polar spacecraft. *Geophysical Research Letters*, *25*, 4063–4066. https://doi.org/10.1029/ 1998GL900071

Lemaire, J. F., & Gringauz, K. I. (1998). *The Earth's plasmasphere*. Cambridge, UK: Cambridge University Press.

Li, W., Shprits, Y. Y., & Thorne, R. M. (2007). Dynamic evolution of energetic outer zone electrons due to wave-particle interactions during storms. *Journal of Geophysical Research*, *112*, A10220. https://doi.org/10.1029/ 2007JA012368

Li, W., Thorne, R. M., Bortnik, J., Tao, X., & Angelopoulos, V. (2012). Characteristics of hiss-like and discrete whistler-mode emissions. *Geophysical Research Letters*, *39*, L18106. https://doi.org/10.1029/2012GL053206

Li, W., Thorne, R. M., Bortnik, J., Reeves, G. D., Kletzing, C. A., Kurth, W. S., … Thaller, S. A. (2013). An unusual enhancement of low-frequency plasmaspheric hiss in the outer plasmasphere associated with substorm-injected electrons. *Geophysical Research Letters*, *40*, 3798–3803. https://doi.org/10.1002/grl.50787

Li, W., Chen, L., Bortnik, J., Thorne, R. M., Angelopoulos, V., Kletzing, C. A., … Hospodarsky, G. B. (2015). First evidence for chorus at a large geocentric distance as a source of plasmaspheric hiss: Coordinated THEMIS and Van Allen Probes observation. *Geophysical Research Letters*, *42*, 241–248. https://doi.org/10.1002/2014GL062832

Liu, K., Winske, D., Gary, S. P., & Reeves, G. D. (2012). Relativistic electron scattering by large amplitude electromagnetic ion cyclotron waves: The role of phase bunching and trapping. *Journal of Geophysical Research*, *117*, A06218. https://doi.org/10.1029/2011JA017476

Liu, N., Su, Z., Gao, Z., Reeves, G. D., Zheng, H., Wang, Y., & Wang, S. (2017). Shock-induced disappearance and subsequent recovery of plasmaspheric hiss: Coordinated observations of RBSP, THEMIS, and POES satellites. *Journal of Geophysical Research: Space Physics*, *122*, 10,421–10,435. https://doi.org/10.1002/2017JA024470

Liu, N., Su, Z., Gao, Z., Zheng, H., Wang, Y., Wang, S., … Wygant, J. R. (2017). Simultaneous disappearances of plasmaspheric hiss, exohiss and chorus waves triggered by a sudden decrease in solar wind dynamic pressure. *Geophysical Research Letters*, *43*, 52–61. https://doi.org/10.1002/2016GL071987

Lyons, L. R., & Thorne, R. M. (1973). Equilibrium structure of radiation belt electrons. *Journal of Geophysical Research*, *78*, 2142–2149. https://doi.org/10.1029/JA078i013p02142

Malaspina, D. M., Jaynes, A. N., Boulé, C., Bortnik, J., Thaller, S. A., Ergun, R. E., … Wygant, J. R. (2016). The distribution of plasmaspheric hiss wave power with respect to plasmapause location. *Geophysical Research Letters*, *43*, 7878–7886. https://doi.org/10.1002/2016GL069982

Malaspina, D. M., Jaynes, A. N., Hospodarsky, G., Bortnik, J., Ergun, R. E., & Wygant, J. (2017). Statistical properties of low-frequency plasmaspheric hiss. *Journal of Geophysical Research: Space Physics*, *122*, 8340–8352. https://doi.org/10.1002/2017JA024328

Mauk, B. H., Fox, N. J., Kanekal, S. G., Kessel, R. L., Sibeck, D. G., & Ukhorskiy, A. (2013). Science objectives and rationale for the Radiation Belt Storm Probes mission. *Space Science Reviews*, *179*, 3–27. https://doi.org/10.1007/s11214-012-9908-y

Meredith, N. P., Thorne, R. M., Horne, R. B., Summers, D., Fraser, B. J., & Anderson, R. R. (2003). Statistical analysis of relativistic electron energies for cyclotron resonance with EMIC waves observed on CRRES. *Journal of Geophysical Research*, *108*(A6), 1250. https://doi.org/10.1029/2002JA009700

Meredith, N. P., Horne, R. B., Thorne, R. M., Summers, D., & Anderson, R. R. (2004). Substorm dependence of plasmaspheric hiss. *Journal of Geophysical Research*, *109*, A06209. https://doi.org/10.1029/2004JA010387

Meredith, N. P., Horne, R. B., Glauert, S. A., & Anderson, R. R. (2007). Slot region electron loss timescales due to plasmaspheric hiss and lightning-generated whistlers. *Journal of Geophysical Research*, *112*, 8214. https://doi.org/10.1029/2007JA012413

Meredith, N. P., Horne, R. B., Bortnik, J., Thorne, R. M., Chen, L., Li, W., & Sicard-Piet, A. (2013). Global statistical evidence for chorus as the embryonic source of plasmaspheric hiss. *Geophysical Research Letters*, *40*, 2891–2896. https://doi.org/10.1002/grl.50593

Mourenas, D., & Ripoll, J.-F. (2012). Analytical estimates of quasi-linear diffusion coefficients and electron lifetimes in the inner radiation belt. *Journal of Geophysical Research*, *117*, A01204. https://doi.org/10.1029/2011JA016985

Nakamura, S., Omura, Y., Summers, D., & Kletzing, C. A. (2016). Observational evidence of the nonlinear wave growth theory of plasmaspheric hiss. *Geophysical Research Letters*, *43*, 10,040–10,049. https://doi.org/10.1002/2016GL070333

Ni, B., Li, W., Thorne, R. M., Bortnik, J., Ma, Q., Chen, L., … Claudepierre, S. G. (2014). Resonant scattering of energetic electrons by unusual low-frequency hiss. *Geophysical Research Letters*, *41*, 1854–1861. https://doi.org/10.1002/2014GL059389

Nishida, A. (1966). Formation of plasmapause, or magnetospheric plasma knee, by the combined action of magnetospheric convection and plasma escape from the tail. *Journal of Geophysical Research*, *71*, 5669–5679. https://doi.org/10.1029/JZ071i023p05669

Nunn, D., Omura, Y., Matsumoto, H., Nagano, I., & Yagitani, S. (1997). The numerical simulation of VLF chorus and discrete emissions observed on the geotail satellite using a Vlasov code. *Journal of Geophysical Research*, *102*, 27,083–27,098. https://doi.org/10.1029/97JA02518

Omura, Y., & Zhao, Q. (2012). Nonlinear pitch-angle scattering of relativistic electrons by EMIC waves in the inner magnetosphere. *Journal of Geophysical Research*, *117*, A08227. https://doi.org/10.1029/2012JA017943

Omura, Y., Furuya, N., & Summers, D. (2007). Relativistic turning acceleration of resonant electrons by coherent whistler mode waves in a dipole magnetic field. *Journal of Geophysical Research*, *112*, A06236. https://doi.org/10.1029/2006JA012243

Omura, Y., Katoh, Y., & Summers, D. (2008). Theory and simulation of the generation of whistler-mode chorus. *Journal of Geophysical Research*, *113*, A04223. https://doi.org/10.1029/2007JA012622

Omura, Y., Nakamura, S., Kletzing, C. A., Summers, D., & Hikishima, M. (2015). Nonlinear wave growth theory of coherent hiss emissions in the plasmasphere. *Journal of Geophysical Research: Space Physics*, *120*, 7642–7657. https://doi.org/10.1002/2015JA021520

Russell, C. T., Holzer, R. E., & Smith, E. J. (1969). OGO 3 observations of ELF noise in the magnetosphere. 1. Spatial extent and frequency of occurrence. *Journal of Geophysical Research*, *74*, 755–777. https://doi.org/10.1029/JA074i003p00755

Santolík, O., Pickett, J. S., Gurnett, D. A., & Storey, L. R. O. (2002). Magnetic component of narrowband ion cyclotron waves in the auroral zone. *Journal of Geophysical Research*, *107*(A12), 1444. https://doi.org/10.1029/2001JA000146

Santolík, O., Parrot, M., & Lefeuvre, F. (2003). Singular value decomposition methods for wave propagation analysis. *Radio Science*, *38*(1), 1010. https://doi.org/10.1029/2000RS002523

Santolík, O., Gurnett, D. A., Pickett, J. S., Parrot, M., & Cornilleau-Wehrlin, N. (2004). A microscopic and nanoscopic view of storm-time chorus on 31 March 2001. *Geophysical Research Letters*, *31*, L02801. https://doi.org/10.1029/2003GL018757

Santolík, O., Pickett, J. S., Gurnett, D. A., Menietti, J. D., Tsurutani, B. T., & Verkhoglyadova, O. (2010). Survey of Poynting flux of whistler mode chorus in the outer zone. *Journal of Geophysical Research*, *115*, A00F13. https://doi.org/10.1029/2009JA014925

Santolík, O., Kletzing, C., Kurth, W., Hospodarsky, G., & Bounds, S. (2014). Fine structure of large-amplitude chorus wave packets. *Geophysical Research Letters*, *41*, 293–299. https://doi.org/10.1002/2013GL058889

Shprits, Y. Y., Subbotin, D., & Ni, B. (2009). Evolution of electron fluxes in the outer radiation belt computed with the VERB code. *Journal of Geophysical Research*, *114*, A11209. https://doi.org/10.1029/2008JA013784

Smith, A. J., & Nunn, D. (1998). Numerical simulation of VLF risers, fallers, and hooks observed in Antarctica. *Journal of Geophysical Research*, *103*(A4), 6771–6784. https://doi.org/10.1029/97JA03396

Solomon, J., Cornilleau-Wehrlin, N., Korth, A., & Kremser, G. (1988). An experimental study of ELF/VLF hiss generation in the Earth's magnetosphere. *Journal of Geophysical Research*, *93*, 1839–1847. https: //doi.org/10.1029/JA093iA03p01839

Sonwalkar, V. S., & Inan, U. S. (1989). Lightning as an embryonic source of VLF hiss. *Journal of Geophysical Research*, *94*, 6986–6994. https://doi.org/10.1029/JA094iA06p06986

Spasojevic, M., Shprits, Y. Y., & Orlova, K. (2015). Global empirical models of plasmaspheric hiss using Van Allen Probes. *Journal of Geophysical Research: Space Physics*, *120*, 10,370–10,383. https://doi.org/10.1002/2015JA021803

Spence, H. E., Reeves, G. D., Baker, D. N., Blake, J. B., Bolton, M., Bourdarie, S., … Thorne, R. M. (2013). Science goals and overview of the Energetic Particle, Composition, and Thermal Plasma (ECT) suite on NASA's Radiation Belt Storm Probes (RBSP) mission. *Space Science Reviews*, *179*, 311–336. https://doi.org/10.1007/s11214-013-0007-5

Su, Z., Xiao, F., Zheng, H., & Wang, S. (2011). CRRES observation and STEERB simulation of the 9 October 1990 electron radiation belt dropout event. *Geophysical Research Letters*, *38*, L06106. https://doi.org/10.1029/2011GL046873

Su, Z., Zhu, H., Xiao, F., Zheng, H., Shen, C., Wang, Y., & Wang, S. (2012). Bounce-averaged advection and diffusion coefficients for monochromatic electromagnetic ion cyclotron wave: Comparison between test-particle and quasi-linear models. *Journal of Geophysical Research*, *117*, A09222. https://doi.org/10.1029/2012JA017917

Su, Z., Zhu, H., Xiao, F., Zheng, H., Shen, C., Wang, Y., & Wang, S. (2013). Latitudinal dependence of nonlinear interaction between electromagnetic ion cyclotron wave and radiation belt relativistic electrons. *Journal of Geophysical Research: Space Physics*, *118*, 3188–3202. https://doi.org/10.1002/jgra.50289

Su, Z., Zhu, H., Xiao, F., Zheng, H., Zhang, M., Liu, Y. C.-M., … Wang, S. (2014). Latitudinal dependence of nonlinear interaction between electromagnetic ion cyclotron wave and terrestrial ring current ions. *Physics of Plasmas*, *21*, 052310. https://doi.org/10.1063/1.4880036

Su, Z., Zhu, H., Xiao, F., Zheng, H., Wang, Y., Shen, C., … Wygant, J. R. (2015). Disappearance of plasmaspheric hiss following interplanetary shock. *Geophysical Research Letters*, *42*, 3129–3140. https://doi.org/10.1002/2015GL063906

Su, Z., Gao, Z., Zhu, H., Li, W., Zheng, H., Wang, Y., … Wygant, J. R. (2016). Nonstorm time dropout of radiation belt electron fluxes on 24 September 2013. *Journal of Geophysical Research: Space Physics*, *121*, 6400–6416. https://doi.org/10.1002/2016JA022546

Su, Z., Gao, Z. L., Zheng, H., Wang, Y., Wang, S., Spence, H. E., … Wygant, J. R. (2017). Rapid loss of radiation belt relativistic electrons by EMIC waves. *Journal of Geophysical Research: Space Physics*, *122*, 9880–9897. https://doi.org/10.1002/2017JA024169

Summers, D., & Omura, Y. (2007). Ultra-relativistic acceleration of electrons in planetary magnetospheres. *Geophysical Research Letters*, *34*, L24205. https://doi.org/10.1029/2007GL032226

Summers, D., Thorne, R. M., & Xiao, F. (1998). Relativistic theory of wave-particle resonant diffusion with application to electron acceleration in the magnetosphere. *Journal of Geophysical Research*, *103*, 20,487–20,500. https://doi.org/10.1029/98JA01740

Summers, D., Ni, B., Meredith, N. P., Horne, R. B., Thorne, R. M., Moldwin, M. B., & Anderson, R. R. (2008). Electron scattering by whistler-mode ELF hiss in plasmaspheric plumes. *Journal of Geophysical Research*, *113*, A04219. https://doi.org/10.1029/2007JA012678

Summers, D., Omura, Y., Nakamura, S., & Kletzing, C. A. (2014). Fine structure of plasmaspheric hiss. *Journal of Geophysical Research: Space Physics*, *119*, 9134–9149. https://doi.org/10.1002/2014JA020437

Thorne, R. M., Smith, E. J., Burton, R. K., & Holzer, R. E. (1973). Plasmaspheric hiss. *Journal of Geophysical Research*, *78*, 1581–1596. https://doi.org/10.1029/JA078i010p01581

Thorne, R. M., Church, S. R., & Gorney, D. J. (1979). On the origin of plasmaspheric hiss—The importance of wave propagation and the plasmapause. *Journal of Geophysical Research*, *84*, 5241–5247. https://doi.org/10.1029/JA084iA09p05241

Thorne, R. M., Li, W., Ni, B., Ma, Q., Bortnik, J., Baker, D. N., … Angelopoulos, V. (2013). Evolution and slow decay of an unusual narrow ring of relativistic electrons near $L\sim3.2$ following the September 2012 magnetic storm. *Geophysical Research Letters*, *40*, 3507–3511. https://doi.org/10.1002/grl.50627

Tsurutani, B. T., & Smith, E. J. (1974). Postmidnight chorus: A substorm phenomenon. *Journal of Geophysical Research*, *79*(1), 118–127. https://doi.org/10.1029/JA079i001p00118

Tsurutani, B. T., Verkhoglyadova, O. P., Lakhina, G. S., & Yagitani, S. (2009). Properties of dayside outer zone chorus during HILDCAA events: Loss of energetic electrons. *Journal of Geophysical Research*, *114*, A03207. https://doi.org/10.1029/2008JA013353

Tsurutani, B. T., Falkowski, B. J., Verkhoglyadova, O. P., Pickett, J. S., SantolíK, O., & Lakhina, G. S. (2012). Dayside ELF electromagnetic wave survey: A Polar statistical study of chorus and hiss. *Journal of Geophysical Research*, *117*, A00L12. https://doi.org/10.1029/2011JA017180

Tsurutani, B. T., Lakhina, G. S., & Verkhoglyadova, O. P. (2013). Energetic electron (>10 keV) microburst precipitation, ∼5-15 s X-ray pulsations, chorus, and wave-particle interactions: A review. *Journal of Geophysical Research: Space Physics*, *118*, 2296–2312. https://doi.org/10.1002/jgra.50264

Tsurutani, B. T., Falkowski, B. J., Pickett, J. S., Verkhoglyadova, O. P., Santolik, O., & Lakhina, G. S. (2014). Extremely intense ELF magnetosonic waves: A survey of polar observations. *Journal of Geophysical Research: Space Physics*, *119*, 964–977. https://doi.org/10.1002/2013JA019284

Tsurutani, B. T., Falkowski, B. J., Pickett, J. S., Santolik, O., & Lakhina, G. S. (2015). Plasmaspheric hiss properties: Observations from Polar. *Journal of Geophysical Research: Space Physics*, *120*, 414–431. https://doi.org/10.1002/2014JA020518

Tsyganenko, N. A., & Sitnov, M. I. (2005). Modeling the dynamics of the inner magnetosphere during strong geomagnetic storms. *Journal of Geophysical Research*, *110*, A03208. https://doi.org/10.1029/2004JA010798

Wang, B., Su, Z., Zhang, Y., Shi, S., & Wang, G. (2016). Nonlinear Landau resonant scattering of near-equatorially mirroring radiation belt electrons by oblique EMIC waves. *Geophysical Research Letters*, *43*, 3628–3636. https://doi.org/10.1002/2016GL068467

Wilson, L., Cattell, C., Kellogg, P., Wygant, J., Goetz, K., Breneman, A., & Kersten, K. (2011). The properties of large amplitude whistler mode waves in the magnetosphere: Propagation and relationship with geomagnetic activity. *Geophysical Research Letters*, *38*, L17107. https://doi.org/10.1029/2011GL048671

Wygant, J., Bonnell, J., Goetz, K., Ergun, R., Mozer, F., Bale, S., … Tao, J. (2013). The electric field and waves instruments on the Radiation Belt Storm Probes mission. *Space Science Reviews*, *179*(1–4), 183–220. https://doi.org/10.1007/s11214-013-0013-7

Yuan, Z., Xiong, Y., Pang, Y., Zhou, M., Deng, X., Trotignon, J. G., … Wang, J. (2012). Wave-particle interaction in a plasmaspheric plume observed by a Cluster satellite. *Journal of Geophysical Research*, *117*, A03205. https://doi.org/10.1029/2011JA017152

Zhu, H., Su, Z., Xiao, F., Zheng, H., Shen, C., Wang, Y., & Wang, S. (2012). Nonlinear interaction between ring current protons and electromagnetic ion cyclotron waves. *Journal of Geophysical Research*, *117*, A12217. https://doi.org/10.1029/2012JA018088

Zhu, H., Su, Z., Xiao, F., Zheng, H., Wang, Y., Shen, C., … Baker, D. N. (2015). Plasmatrough exohiss waves observed by Van Allen Probes: Evidence for leakage from plasmasphere and resonant scattering of radiation belt electrons. *Geophysical Research Letters*, *42*, 1012–1019. https://doi.org/10.1002/2014GL062964